

Dynamical lattice QCD studies of hadron structure

Ph. Hägler^a

^aInstitut für Theoretische Physik T39, Physik-Department der TU München, 85747 Garching, Germany

Dynamical lattice QCD studies of form factors, moments of PDFs and GPDs, and many other important observables have seen impressive progress during recent years. They allow us to address a number of fundamental physics questions, for example related to the distribution of charge and momentum inside hadrons and the decomposition of the nucleon spin. This talk illustrates the recent achievements and remaining challenges by reviewing a small selection of lattice hadron structure results.

1. INTRODUCTION

The remarkable efforts during the last decades in theoretical and experimental studies of elastic and deeply inelastic lepton-hadron scattering and related processes have provided detailed insights into many aspects of the structure of the nucleon. Complementary to these efforts, lattice QCD represents an excellent tool to investigate many fundamental hadron properties from first principles. Quantities which have been measured experimentally to a high precision, for example the axial vector coupling constant g_A or the nucleon magnetic moment μ , may be regarded as benchmark observables and indeed still pose a significant challenge for lattice calculations, see, e.g., [1–3]. In other cases, for example with respect to the energy momentum tensor and quark helicity flip (generalized) form factors, the lattice approach has distinct advantages over phenomenological studies, and provides already now great additional insight into the quark substructure of hadrons [4–7].

As will become clear in the following sections, even the lattice hadron structure calculations at comparatively low pion masses of ≈ 300 MeV that have been reached in recent years still require highly non-trivial extrapolations to the physical point. Therefore solid predictions from chiral perturbation theory for the pion mass (and ideally also volume) dependence of the lattice data are of crucial importance.

Below, we begin with a short overview of dynamical lattice calculations of the pion and the

nucleon charge radius. This is followed by an update on results for moments of generalized parton distributions (GPDs) and the nucleon spin sum rule from the LHP collaboration. Finally, we present a first exploratory lattice study of transverse momentum dependent PDFs. For more detailed reviews of lattice hadron structure calculations, we refer to [8–11].

2. ELECTROMAGNETIC FORM FACTORS AND CHARGE RADII

2.1. The pion

Significant progress, mostly based on combinations of new methods and techniques, has been made in recent years with respect to lattice calculations of the pion electromagnetic form factor $F_\pi(Q^2)$, see, e.g., Refs. [12–16]. An illustrative example is the work by the RBC-UKQCD collaboration [16] that is based on $n_f = 2 + 1$ flavors of domain wall fermions, with a pion mass of $m_\pi = 330$ MeV, a lattice spacing of $a \approx 0.114$ fm, and a volume of $V \approx (2.74 \text{ fm})^3$. In that study, the cost of the calculations was significantly reduced, and a high precision achieved, by using random wall sources instead of the conventional point sources for the computation of the quark propagators. Most importantly, very small, non-zero values of the momentum transfer in the range $Q^2 \approx 0.01, \dots, 0.04 \text{ GeV}^2$ have been accessed by employing so-called partially twisted boundary conditions [17,18]. It is remarkable that the smallest non-zero Q^2 reached in this lattice calculation is below the lowest Q^2 that could be so

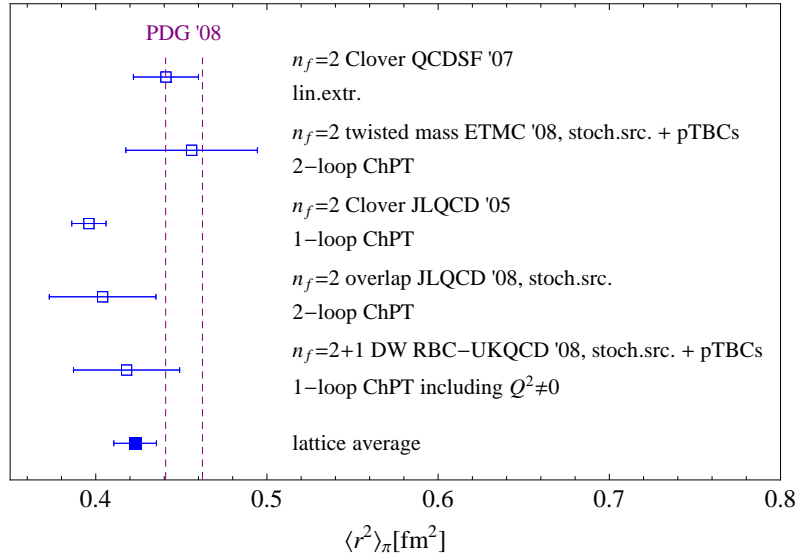


Figure 1. Overview of dynamical lattice QCD results for the chirally extrapolated pion mean square radius at the physical pion mass (references are provided in the text).

far accessed in experimental studies of $F_\pi(Q^2)$. Finally, from a chiral fit to the lattice data points using the original chiral perturbation theory result by Gasser and Leutwyler for $F_\pi(Q^2)$ [19], a pion charge radius of $\langle r_\pi^2 \rangle = 0.418(31) \text{ fm}^2$ was found at the physical pion mass. This value is shown and compared to other recent lattice results and the experimental value in Fig. 1. Noting that the lattice values were obtained for a number of different lattice actions and chiral extrapolations, it is encouraging to see that they mostly agree within errors. It will be interesting to track down the origin of the slight discrepancy between the lattice average and experiment in future studies of the pion form factor.

2.2. The nucleon

During the recent years, a number of dynamical lattice calculations of the nucleon form factors were performed by different collaborations, with pion masses as low as $\approx 300 \text{ MeV}$ [20–25]. A fundamental observable derived from form factors is the mean square (ms) radius $\langle r^2 \rangle \propto -(dF(Q^2)/dQ^2)_{Q^2=0}$. Figure 2 gives on

overview of results for the isovector Dirac ms radius $\langle r_1^2 \rangle_{u-d}$ as a function of the pion mass. Overall, the lattice data points obtained for the different actions and for $N_f = 2$ and $N_f = 2 + 1$ flavors are in good agreement within the statistical errors. Although the lattice values are slowly increasing towards smaller pion masses, they are still almost a factor of two below the phenomenological values, even at the lowest accessible lattice pion masses. Notwithstanding possible systematic uncertainties, this indicates that a strong chiral dynamics has to set in for $m_\pi < 300 \text{ MeV}$, and ChPT calculations indeed predict that $\langle r_1^2 \rangle$ rises as $\ln(m_\pi)$ towards the chiral limit, as illustrated by the curves in Fig. 2. It is a major challenge to numerically demonstrate the presence of the predicted chiral singularity in lattice calculations at lower pion masses.

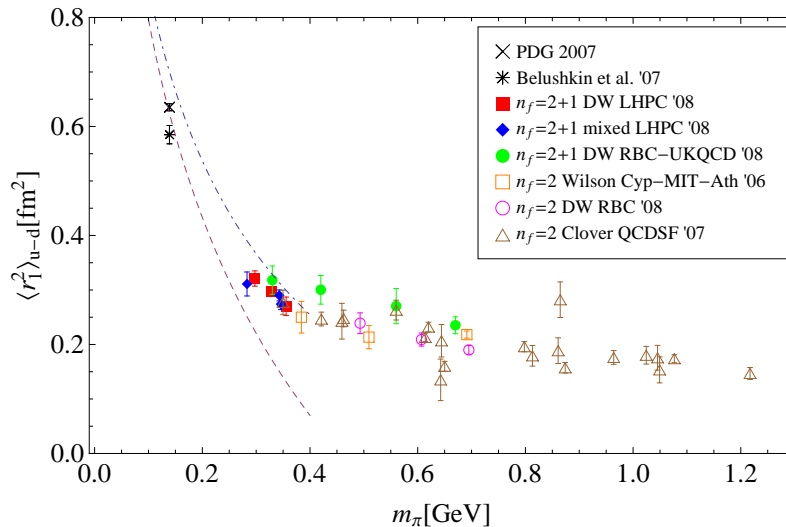


Figure 2. Overview of dynamical lattice QCD results for the isovector Dirac mean square radius (references are provided in the text). The dashed curve represents the leading 1-loop HBChPT prediction [26], and the dotted-dashed curve the result obtained in the SSE [27].

3. MOMENTS OF GPDs AND THE DECOMPOSITION OF THE NUCLEON SPIN

One of the main motivations for the study of nucleon GPDs $H(x, \xi, t)$, $E(x, \xi, t)$, \dots (for reviews, see [28–30]) is their direct relation to the nucleon spin sum rule. As has already been shown in [31], the nucleon spin can be decomposed as

$$\begin{aligned} \frac{1}{2} &= \frac{1}{2}(A(0) + B(0)) = \frac{1}{2} \left(\sum_q \langle x \rangle_q + \langle x \rangle_g \right) \\ &+ \sum_q B_{20}^q(0) + B_{20}^g(0) \equiv \sum_q J_q + J_g, \end{aligned} \quad (1)$$

and is therefore, in addition to the momentum fractions $\langle x \rangle$ carried by the quarks and gluons, fully determined by the form factors $B_{q,g}(t)$ of the energy-momentum tensor at vanishing momentum transfer, $t = 0$ ¹. It turns out that the

¹ $B_{q,g}(t = 0)$ is also known as *anomalous gravitomagnetic moment* [32,33] and has to vanish identically when summed over quarks and gluons, $\sum_{q,g} B(0) = 0$.

form factors $B_{q,g}(t)$ are identical to the second x -moments of the GPDs $E^{q,g}(x, \xi, t)$ at $\xi = 0$,

$$B_{q,g}(t) = \int_{-1}^1 dx x E^{q,g}(x, \xi = 0, t). \quad (2)$$

Furthermore, the total angular momentum of quarks can be naturally decomposed in a gauge-invariant manner in terms of quark spin and orbital angular momentum contributions, $J_q = \Delta\Sigma/2 + L_q$. Substantial progress has been made since the first lattice QCD calculations of moments of GPDs by the LHPC and QCDSF collaborations in 2003 [34,35]. The so far most comprehensive lattice study of GPDs has been presented in [7] by LHPC based on a mixed action approach, which has been updated recently by inclusion of an additional ensemble at a lower pion mass of $m_\pi \approx 300$ MeV and by an increase in statistics by a factor of 8 [36]. Together with corresponding results for the quark spin fraction $\Delta\Sigma/2$, the lattice data for the form factors $A(t)$ and $B(t)$ was used to calculate the OAM carried by the quarks, displayed in Fig. 3 for $(u+d)$ -quarks as a function of m_π^2 . Results from a covariant chiral perturba-

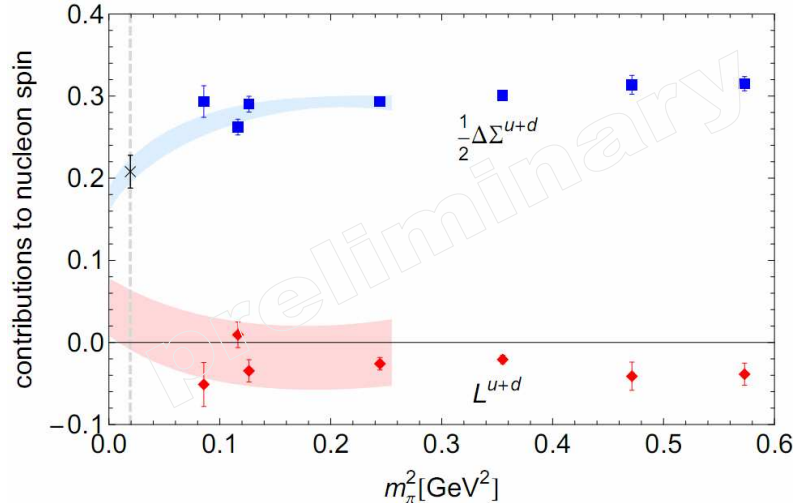


Figure 3. Contributions to the nucleon spin in the $\overline{\text{MS}}$ scheme at a scale of $\mu = 2$ GeV.

tion theory calculation [37] were employed to simultaneously extrapolate the energy momentum tensor form factors to $t = 0$ and the physical pion mass. This was combined with a heavy baryon ChPT fit of $\Delta\Sigma/2$ to obtain a chiral extrapolation of L^{u+d} , as illustrated by the error bands in Fig. 3. While the total quark spin turns out to be in very good agreement with results from HERMES [38], a very small OAM contribution of only $L^{u+d} \approx (5 \pm 5)\%$ is found at the physical pion mass. This is at first sight in striking disagreement with common expectations, based for example on relativistic quark models, which predict that the quark OAM amounts to $\approx 30 - 40\%$ of the total nucleon spin. Furthermore, on quite general grounds a non-zero quark orbital angular momentum is required for the Pauli form factor F_2 to be non-vanishing, and also for the existence of certain single spin asymmetries, related to e.g. the Sivers effect, in semi-inclusive scattering processes [33,39,40].

The solution to these apparent puzzles is at least two-fold. First of all, we note that a small total, $u+d$, OAM contribution does not necessarily imply that the individual up and down quark orbital angular momenta are non-zero, since L^q

is not bound to be positive. First evidence in this direction comes from the anomalous magnetic moments of the proton and the neutron, $\kappa_{p,n} = F_2^{p,n}(0)$, which are separately large in magnitude. However, taking into account isospin symmetry, one finds that the contributions from up and down quarks to κ_p cancel out to a large extent in the sum, $\kappa_p^{u+d} \approx -0.36$. Inspired by this observation, we show in Fig. 4 the individual up and down quark spin and OAM contributions to the nucleon spin as functions of m_π^2 , together with corresponding chiral extrapolations given by the error bands. Indeed, it turns out that the orbital angular momenta of up and down quarks are both large and very similar in magnitude, but opposite in sign, over a wide range of accessible pion masses, and therefore nearly cancel in the sum. From the chiral extrapolations, we find that the quarks carry a substantial amount of OAM of $|L^{u,d}| \approx 33\%$ at the physical pion mass.

What remains to be understood is the discrepancy between the lattice observation of a nearly zero total quark OAM, $L^{u+d} \approx 0$, and the model expectation that $L^{u+d} \approx 40\%$. In this respect, it has been noted that the model calculations generically correspond to a low hadronic scale

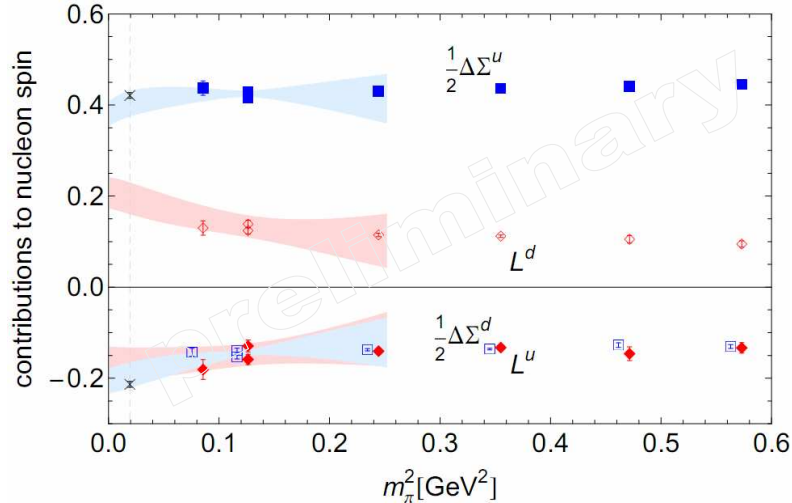


Figure 4. Contributions from up and down quarks to the nucleon spin in the $\overline{\text{MS}}$ scheme at a scale of $\mu = 2$ GeV.

$\ll 1$ GeV, while the lattice scale is typically ≈ 2 GeV (with lattice results usually transformed to the $\overline{\text{MS}}$ -scheme) [41,42]. A naive, direct comparison of lattice and model results is therefore in general meaningless. Instead, one might attempt to employ QCD evolution to evolve the lattice values down to the lower model scale. This is displayed in Fig. 5 using NLO evolution. Indeed, the quark OAM increases substantial at lower scales, and a very good agreement with relativistic quark model results is found at the model scale, which has been fixed to the value at which the gluon contribution vanishes, $J_g = 0$ (indicated by the dashed vertical line in Fig. 5).

4. TRANSVERSE NUCLEON SPIN STRUCTURE FROM TMDs

Another important class of observables is given by the so-called transverse momentum dependent parton distribution functions (TMDs). They encode fundamental information about hadron structure that is mostly complementary to the physics content of PDFs and GPDs. TMDs are generically denoted by $[f, g, h](x, k_\perp^2)$, and depend, in addition to the longitudinal momentum

fraction x , also on the intrinsic transverse momentum k_\perp carried by the partons. They have in general a probability density interpretation (for issues related to the high- k_\perp behavior and the integrability of TMDs we refer to [43]), similar to the generalized parton distributions (GPDs) in impact parameter (b_\perp)-space [44]. It is interesting to note that although the transverse momentum, k_\perp , and the coordinate, b_\perp , are *not* Fourier-conjugated variables, a number of *approximate* relations between TMDs and GPDs have been established and conjectured [45–47]. TMDs play a central role in the phenomenology of semi-inclusive deep inelastic scattering (SIDIS) and the Drell-Yan-process, where correlations between the intrinsic transverse momenta of the partons, the hadron momenta, and their spins lead to a variety of interesting asymmetries. A lot of attention has been attracted by the Sivers- and Collins-effect [48,49], which give rise to single spin azimuthal asymmetries in SIDIS, and which have already been studied experimentally at HERMES, COMPASS and BELLE [50–52].

Recently, we have performed a first exploratory lattice QCD study of k_\perp -distributions [53–55].

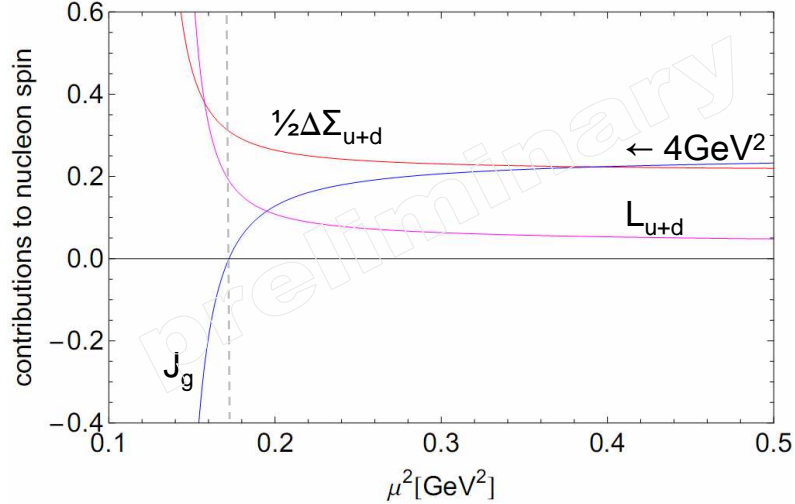


Figure 5. Evolution of contributions to the nucleon spin.

The calculations were based on (nucleon matrix elements of) manifestly non-local, gauge invariant quark operators, giving access to a number of invariant amplitudes. We note that due to our particular choice of “process-independent” non-local lattice operators, the lattice results should not be quantitatively compared with phenomenological studies of TMDs performed in, e.g., [56,57].

The numerical lattice results for the amplitudes can in turn be parametrized and then Fourier-transformed to obtain the k_{\perp} -distributions. A very useful interpretation of the various k_{\perp} -dependent PDFs can be given in form of quark densities in the transverse momentum plane. The density of longitudinally polarized quarks with helicity λ in a nucleon with helicity Λ or transverse spin \mathbf{S}_{\perp} is given by [46]

$$\rho_L = \frac{1}{2} \left(f_1 + \lambda \Lambda g_1 + \left[\frac{\mathbf{S}_j \epsilon_{j i} \mathbf{k}_i}{m_N} f_{1T}^{\perp} \right] + \lambda \frac{\mathbf{k}_{\perp} \cdot \mathbf{S}_{\perp}}{m_N} g_{1T} \right), \quad (3)$$

while for transversely polarized quarks with spin \mathbf{s}_{\perp} in a longitudinally polarized nucleon one finds [46]

$$\rho_T = \frac{1}{2} \left(f_1 + \mathbf{s}_{\perp} \cdot \mathbf{S}_{\perp} h_1 + \left[\frac{\mathbf{s}_j \epsilon_{j i} \mathbf{k}_i}{m_N} h_1^{\perp} \right] + \frac{\mathbf{s}_j (2\mathbf{k}_j \mathbf{k}_i - \mathbf{k}_{\perp}^2 \delta_{j i}) \mathbf{S}_i}{2m_N^2} h_{1T}^{\perp} + \Lambda \frac{\mathbf{k}_{\perp} \cdot \mathbf{s}_{\perp}}{m_N} h_{1L}^{\perp} \right). \quad (4)$$

Notably, both densities have the form of a multipole-expansion, with monopole terms $\propto f_1, g_1, h_1$, dipole structures $\propto f_{1T}^{\perp}, g_{1T}, h_1^{\perp}, h_{1L}^{\perp}$, and a quadrupole term $\propto h_{1T}^{\perp}$. We note that all TMDs in Eqs. 3,4 depend on x and k_{\perp}^2 , and that the terms in square brackets are absent for our choice of non-local lattice operators [55]. The lattice results for the lowest x -moment of the densities are illustrated in Fig. 6 for up- and down-quarks on the left and the right, respectively. The density $\rho_L(x, k_{\perp})$ is displayed in the upper half for $\lambda = +1$ and $\mathbf{S}_{\perp} = (1, 0)$, while the lower half of Fig. 6 shows $\rho_T(x, k_{\perp})$ for $\mathbf{s}_{\perp} = (1, 0)$ and $\Lambda = +1$. Due to the non-zero lattice results for the distributions $g_{1T}^u > 0$, $g_{1T}^d < 0$, and $h_{1L}^{\perp, u} < 0$, $h_{1L}^{\perp, d} > 0$ in particular, we observe significant correlations between the quark and nucleon spins and the intrinsic quark transverse momentum, leading to clearly visible dipole deformations in

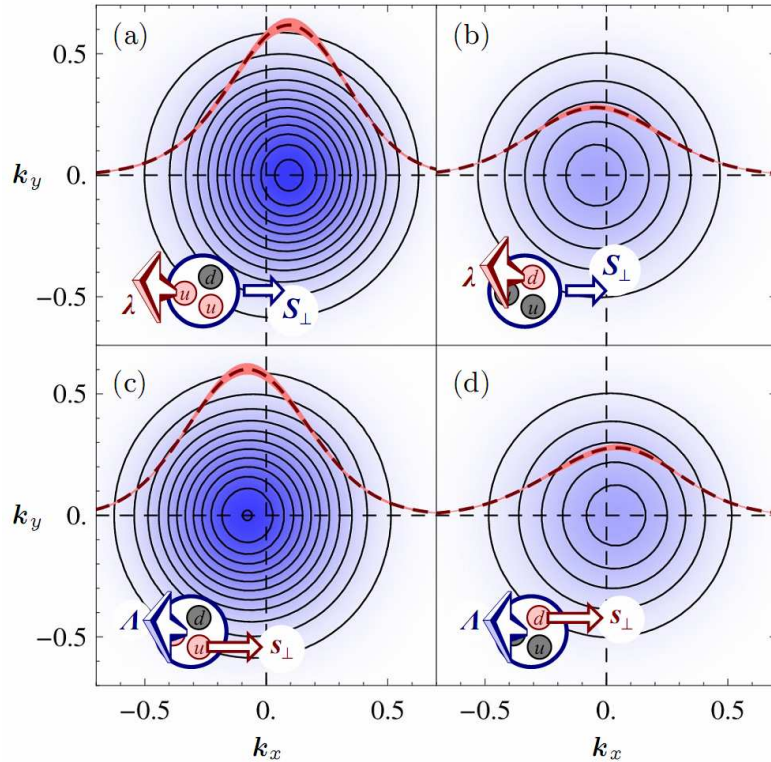


Figure 6. Transverse momentum densities of up (on the left) and down (on the right) quarks in the nucleon (from [55]).

opposite directions for up- and for down-quarks in Fig. 6. Since the distributions g_{1T} , h_{1L}^\perp have, in contrast to nearly all others TMDs, no analogs in the framework of GPDs due to time reversal symmetry [46], the deformations may be seen as a genuine effect of intrinsic k_\perp of quarks in the nucleon. Our findings for the signs and overall magnitudes of the up and down quark contributions to g_{1T} and h_{1L}^\perp are in good agreement with recent light-cone quark model calculations [58]. Finally, we note that it is very illustrative to contrast the k_\perp -densities in Fig. 6 with lattice results for impact-parameter (b_\perp -) densities based on moments of GPDs, presented in [5] for the nucleon, and in [6] for the pion.

5. SUMMARY

We have illustrated the remarkable progress that has been made in dynamical lattice QCD investigations of hadron structure in the recent years by discussing a selected number of results related to hadron form factors, moments of generalized parton distributions, and transverse momentum dependent PDFs. Lattice calculations of the pion electromagnetic form factor, in combination with ChPT, have reached an accuracy and a precision that allows already today for a meaningful, direct comparison with experiment. The Dirac and Pauli mean square nucleon radii at the lowest accessible pion masses of $m_\pi \approx 300$ MeV on the lattice are still a factor of about two below the experimental numbers. Substantially im-

proved calculations at even lower pion masses and in larger lattice volumes will be necessary to verify the existence of the logarithmic and linear divergences in $\langle r_1^2 \rangle$ and $\langle r_2^2 \rangle$, respectively, in the limit $m_\pi \rightarrow 0$, as predicted by ChPT. Remarkable lattice QCD studies of the gravitational form factors of the nucleon provide important insights into Ji's nucleon spin sum rule, pointing for example towards a very small total orbital angular momentum contribution from quarks. Finally, we have seen a first exploratory lattice calculation of transverse momentum densities, which turn out to be visibly deformed for polarized quarks in a polarized nucleon due to strong correlations between the transverse spins and the intrinsic k_\perp carried by the quarks.

6. Acknowledgments

It is a pleasure to thank M. Altenbuchinger, B. Musch and W. Weise from the theory group T39 at the TU München, and the colleagues from the LHPC and the QCDSF collaborations. I gratefully acknowledge the support by the Emmy-Noether program and the cluster of excellence "Origin and Structure of the Universe" of the DFG.

REFERENCES

1. LHPC, R.G. Edwards et al., Phys. Rev. Lett. 96 (2006) 052001, hep-lat/0510062.
2. A.A. Khan et al., Phys. Rev. D74 (2006) 094508, hep-lat/0603028.
3. S.N. Syritsyn et al., (2009), 0907.4194.
4. QCDSF, M. Göckeler et al., Phys. Lett. B627 (2005) 113, hep-lat/0507001.
5. QCDSF, M. Göckeler et al., Phys. Rev. Lett. 98 (2007) 222001, hep-lat/0612032.
6. QCDSF, D. Brömmel et al., Phys. Rev. Lett. 101 (2008) 122001, 0708.2249.
7. LHPC, P. Hägler et al., Phys. Rev. D77 (2008) 094502, 0705.4295.
8. K. Orginos, PoS LAT2006 (2006) 018.
9. P. Hägler, PoS LAT2007 (2007) 013, 0711.0819.
10. J.M. Zanotti, PoS LAT2008 (2008) 007, 0812.3845.
11. A. Schäfer, Nucl. Phys. A805 (2008) 230.
12. JLQCD, S. Hashimoto et al., PoS LAT2005 (2006) 336, hep-lat/0510085.
13. QCDSF/UKQCD, D. Brömmel et al., Eur. Phys. J. C51 (2007) 335, hep-lat/0608021.
14. R. Frezzotti, V. Lubicz and S. Simula, (2008), 0812.4042.
15. TWQCD, JLQCD et al., (2008), 0810.2590.
16. P.A. Boyle et al., JHEP 07 (2008) 112, 0804.3971.
17. C.T. Sachrajda and G. Villadoro, Phys. Lett. B609 (2005) 73, hep-lat/0411033.
18. P.F. Bedaque and J.W. Chen, Phys. Lett. B616 (2005) 208, hep-lat/0412023.
19. J. Gasser and H. Leutwyler, Ann. Phys. 158 (1984) 142.
20. C. Alexandrou et al., Phys. Rev. D74 (2006) 034508, hep-lat/0605017.
21. QCDSF, M. Göckeler et al., (2007), 0709.3370.
22. LHPC, S. Syritsyn et al., PoS LAT2008 (2008) 169.
23. J.D. Bratt et al., PoS LATTICE2008 (2008) 141, 0810.1933.
24. H.W. Lin et al., Phys. Rev. D78 (2008) 014505, 0802.0863.
25. for RBC and UKQCD, S. Ohta and T. Yamazaki, (2008), 0810.0045.
26. V. Bernard et al., Nucl. Phys. B388 (1992) 315.
27. QCDSF, M. Göckeler et al., Phys. Rev. D71 (2005) 034508, hep-lat/0303019.
28. K. Goeke, M.V. Polyakov and M. Vanderhaeghen, Prog. Part. Nucl. Phys. 47 (2001) 401, hep-ph/0106012.
29. M. Diehl, Phys. Rept. 388 (2003) 41, hep-ph/0307382.
30. A.V. Belitsky and A.V. Radyushkin, Phys. Rept. 418 (2005) 1, hep-ph/0504030.
31. X.D. Ji, Phys. Rev. Lett. 78 (1997) 610, hep-ph/9603249.
32. O.V. Teryaev, (1999), hep-ph/9904376.
33. S.J. Brodsky et al., Nucl. Phys. B593 (2001) 311, hep-th/0003082.
34. LHPC, P. Hägler et al., Phys. Rev. D68 (2003) 034505, hep-lat/0304018.
35. QCDSF, M. Göckeler et al., Phys. Rev. Lett. 92 (2004) 042002, hep-ph/0304249.

36. LHPC, in preparation, 2009.
37. M. Dorati, T.A. Gail and T.R. Hemmert, Nucl. Phys. A798 (2008) 96, nucl-th/0703073.
38. HERMES, A. Airapetian et al., Phys. Rev. D75 (2007) 012007.
39. S.J. Brodsky, D.S. Hwang and I. Schmidt, Phys. Lett. B530 (2002) 99, hep-ph/0201296.
40. M. Burkardt and D.S. Hwang, Phys. Rev. D69 (2004) 074032, hep-ph/0309072.
41. M. Wakamatsu and Y. Nakakoji, Phys. Rev. D77 (2008) 074011, 0712.2079.
42. A.W. Thomas, Phys. Rev. Lett. 101 (2008) 102003, 0803.2775.
43. A. Bacchetta et al., JHEP 08 (2008) 023, 0803.0227.
44. M. Burkardt, Phys. Rev. D62 (2000) 071503, hep-ph/0005108.
45. M. Burkardt, Phys. Rev. D66 (2002) 114005, hep-ph/0209179.
46. M. Diehl and P. Hägler, Eur. Phys. J. C44 (2005) 87, hep-ph/0504175.
47. S. Meissner, A. Metz and K. Goeke, Phys. Rev. D76 (2007) 034002, hep-ph/0703176.
48. D.W. Sivers, Phys. Rev. D41 (1990) 83.
49. J.C. Collins, Nucl. Phys. B396 (1993) 161.
50. HERMES, A. Airapetian et al., Phys. Rev. Lett. 94 (2005) 012002, hep-ex/0408013.
51. COMPASS, V.Y. Alexakhin et al., Phys. Rev. Lett. 94 (2005) 202002, hep-ex/0503002.
52. Belle, K. Abe et al., Phys. Rev. Lett. 96 (2006) 232002, hep-ex/0507063.
53. B.U. Musch et al., (2008), 0811.1536.
54. B. Musch, PhD thesis, TU Munich, 2009.
55. P. Hägler et al., (2009), 0908.1283.
56. M. Anselmino et al., Phys. Rev. D 71 (2005) 074006.
57. A. Bianconi and M. Radici, Phys. Rev. D73 (2006) 114002.
58. B. Pasquini, S. Cazzaniga and S. Boffi, Phys. Rev. D78 (2008) 034025.